

# PROCEEDINGS OF SPIE

[SPIDigitalLibrary.org/conference-proceedings-of-spie](https://spiedigitallibrary.org/conference-proceedings-of-spie)

## Transcranial direct current stimulation transiently increases the blood-brain barrier solute permeability in vivo

Shin, Da Wi, Khadka, Niranjana, Fan, Jie, Bikson, Marom, Fu, Bingmei

Da Wi Shin, Niranjana Khadka, Jie Fan, Marom Bikson, Bingmei M. Fu, "Transcranial direct current stimulation transiently increases the blood-brain barrier solute permeability in vivo," Proc. SPIE 9788, Medical Imaging 2016: Biomedical Applications in Molecular, Structural, and Functional Imaging, 97881X (29 March 2016); doi: 10.1117/12.2218197

**SPIE.**

Event: SPIE Medical Imaging, 2016, San Diego, California, United States

# Transcranial direct current stimulation transiently increases the blood-brain barrier solute permeability in vivo

Da Wi Shin, Niranjana Khadka, Jie Fan, Marom Bikson and Bingmei M. Fu<sup>\*</sup>  
Department of Biomedical Engineering, The City College of the City University of New York  
160 Convent Ave, New York, NY 10031

## ABSTRACT

Transcranial Direct Current Stimulation (tDCS) is a non-invasive electrical stimulation technique investigated for a broad range of medical and performance indications. Whereas prior studies have focused exclusively on direct neuron polarization, our hypothesis is that tDCS directly modulates endothelial cells leading to transient changes in blood-brain-barrier (BBB) permeability (P) that are highly meaningful for neuronal activity. For this, we developed state-of-the-art imaging and animal models to quantify P to various sized solutes after tDCS treatment. tDCS was administered using a constant current stimulator to deliver a 1mA current to the right frontal cortex of rat (approximately 2 mm posterior to bregma and 2 mm right to sagittal suture) to obtain similar physiological outcome as that in the human tDCS application studies. Sodium fluorescein (MW=376), or FITC-dextran (20K and 70K), in 1% BSA mammalian Ringer was injected into the rat (SD, 250-300g) cerebral circulation via the ipsilateral carotid artery by a syringe pump at a constant rate of ~3 ml/min. To determine P, multiphoton microscopy with 800-850 nm wavelength laser was applied to take the images from the region of interest (ROI) with proper microvessels, which are 100-200 micron below the pia mater. It shows that the relative increase in P is about 8-fold for small solute, sodium fluorescein, ~35-fold for both intermediate sized (Dex-20k) and large (Dex-70k) solutes, 10 min after 20 min tDCS pretreatment. All of the increased permeability returns to the control after 20 min post treatment. The results confirmed our hypothesis.

**Keywords:** Blood-Brain Barrier, Transcranial Direct Current Stimulation, Multiphoton microscopy, BBB permeability to small and large molecules, Rat brain, in vivo

## 1. INTRODUCTION

The blood-brain barrier (BBB) plays a major role in protecting the brain from harmful substances in the circulating blood. To serve as a protecting barrier, the BBB is formed by endothelial cells with tight junctions between endothelial cells, which are additionally wrapped by perivascular structures such as astrocytes and pericytes as well as basal membrane<sup>1</sup>. In normal brain, the BBB highly restricts the passage of compounds so the homeostasis within the sensitive environment of the brain parenchyma can be maintained. The barrier is slightly permeable to ions such as sodium, potassium and chloride, but large molecules, such as proteins and most water-soluble chemicals only pass poorly<sup>2</sup>. In order to deliver therapeutic drugs into the central nervous system for the treatment of brain disorders, therefore, it is important to develop non-invasive methods which can temporarily enhance the BBB permeability<sup>3</sup>.

Previous studies have shown that various methods, including focused ultrasound and intra-arterial injection of mannitol, succeeded in transiently increasing the BBB permeability<sup>4,5,6</sup>. However, in searching for a more effective non-invasive method that can transiently increase the BBB permeability, transcranial direct current stimulation (tDCS) seemed promising and very clinically applicable. At appropriate current dosage and application location, tDCS may achieve non-invasive, selective, and localized disruption of the BBB without damages to the brain tissue.

In addition, understanding the cellular mechanisms of tDCS will increase the rigor and efficacy on research for any application of tDCS. A concept of tDCS is that it “primes” the brain somehow increasing “neuronal capacity” and the ability to learn an associated task<sup>7,8</sup>. Notably though various protocols are used, and they can broadly be classified as (A) applying tDCS during a task (typical in cognitive neuroscience) or (B) applying tDCS prior to the task (typical in rehabilitation). Evidences for tDCS directly changing neuronal excitability and capacity for plasticity have been established in human and brain slice models<sup>9</sup>, however, the effect of tDCS on the blood-brain barrier (BBB) is absent.

Since the BBB regulates the neuronal microenvironment, which in turn would profoundly influence “neuronal capacity”, it is thus necessary to investigate the neurovascular coupling under the treatment of tDCS.

Other forms of electrical stimulation which can directly change vascular function have been known<sup>10, 11, 12</sup>, including work by our group applying Deep Brain Stimulation waveforms to endothelial monolayers<sup>13</sup>, in the absence of neurons. This model system proves a direct effect on the endothelial barrier of the BBB. The most evident physiological outcome of direct current stimulation (DCS) is skin erythema<sup>14</sup>, which has a dose response and persistence broadly comparable to the neurophysiological effects of tDCS. Cellular changes produced by DCS on endothelial cells have been characterized<sup>15, 16, 17</sup>, including re-orientation and secretion of growth factors and nitric oxide<sup>18</sup>. tDCS has been shown to change cerebral perfusion in human<sup>19, 20, 21</sup> and animals<sup>22</sup>, though in vivo data from fMRI cannot distinguish between the changes in the BBB function secondary to neuronal stimulation or direct electrical stimulation of the BBB due to the relatively low spatial resolution of fMRI<sup>23, 24</sup>, in which the highest resolution is ~100µm/pixel, much beyond the sub-micron meter resolution required for determining the BBB permeability.

Changes in BBB are known to influence the neuronal microenvironment and so brain function. The BBB tightly regulates the neuronal microenvironment including the excitability and metabolic capacity of neurons. Thus, our goal in this study is to utilize our multiphoton microscopy<sup>25</sup> to quantitatively assess the tDCS-induced BBB permeability change in vivo. In addition to the sub-micron meter spatial resolution, multiphoton microscopy offers the advantage of deep tissue penetration, which is essential for the BBB permeability measurement. The used current dosage, duration and application location of the tDCS were based on previous studies. After tDCS treatment, each of various solutes were injected via the carotid artery, and the BBB permeability was determined for individual microvessels by a method described by Yuan et al<sup>26</sup>.

## 2. METHODS

### 2.1 Animal Preparation

Adult female Sprague Dawley rats (250–300 g, age 3–4 months; Hilltop Laboratory Animals Inc., Scottsdale, PA, USA) were used to conduct in vivo experiments. All procedures and the animals use were approved by the Institutional Animal Care and Use Committee of the City College of New York. Rats were anesthetized with pentobarbital sodium injected subcutaneously. The initial dosage was 65 mg/kg per bodyweight. A heating pad was used to keep the rat at its body temperature throughout the entire experiment. The depth of anesthesia was monitored for the absence of withdrawal reflex to toe pinch and absence of blink reflex. Anesthesia was further checked every 15 minutes during the experiment; an additional 3 mg/dose pentobarbital was given when needed. At the end of the experiments, an overdose of pentobarbital (>100 mg/kg) was administered intravenously to euthanize the animal.

The preparation of the rat skull observation area was the same as that previously described (Shi et al., 2014; Yuan et al., 2009)<sup>35, 37</sup>. Briefly, the skull in the region of interest (ROI) was exposed by shaving off the hair and cutting away the skin and connective tissue. A section of the frontoparietal bone (either left or right) was carefully ground with a high speed micro-grinder (0–50,000 rpm, DLT 50KBU; Brasseler USA, Savannah, GA, USA) until a part of it (~4 mm x 6 mm) became soft and translucent. During the process, artificial CSF (ACSF) at room temperature was applied to the surface of the skull to dispel the heat due to grinding. After grinding, the left or the right carotid artery was cannulated with PE50 tubing. The rat was then placed on a stereotaxic alignment system (SAS 597; David Kopf Instruments, Tujunga, CA, USA), and its head was fixed with two ear bars and a mouth clamp. After tDCS treatment for 20 min, the cerebral microvessels were observed under the objective lens of a multiphoton microscope through the thinned part of the skull and the BBB permeability was determined (**Fig. 1**).

### 2.2 Solutions and fluorescent test solute

#### 2.2.1 Mammalian ringer's solution

Mammalian Ringer's solution was used for all perfusates, which was composed of (in mM) NaCl 132, KCl 4.6, MgSO<sub>4</sub> 1.2, CaCl<sub>2</sub> 2.0, NaHCO<sub>3</sub> 5.0, glucose 5.5, and HEPES 20. The pH was buffered to 7.40–7.45 by adjusting the ratio of HEPES acid to base. In addition, both the washout solution and the fluorescent dye solution contained 10 mg/mL BSA (A4378; Sigma-Aldrich)<sup>26</sup>. The solutions were made fresh on the day of use to avoid binding to the serum albumin.

### 2.2.2 ACSF

The ACSF solution composition was (in mM) NaCl 110.5, KCl 4.7, CaCl<sub>2</sub> 2.5, KH<sub>2</sub>PO<sub>4</sub> 1.1, MgSO<sub>4</sub>·7H<sub>2</sub>O 1.25, NaHCO<sub>3</sub> 25, and HEPES 15<sup>27</sup>, and the solution was buffered to pH 7.4±0.5.

### 2.2.3 Fluorescent solutes

Both FITC-dextran, FITC-dextran-20k (FD20 s, Sigma; mol. wt. 20,000, Stokes radius ~2.4 nm) and FITC-dextran-70k (FD70 s, Sigma; mol. wt. 70,000, Stokes radius ~3.6 nm) were dissolved at 1 mg/ml, Sodium fluorescein (F6377, Sigma; mol. wt. 376, Stokes–Einstein radius ~0.45 nm) was dissolved at 0.1 mg/ml in the Ringer solution containing 10 mg/ml BSA.

## 2.3 Transcranial direct current stimulation (tDCS)

tDCS was administered using a constant current stimulator (1x1 tDCS, Soterix Medical Inc, New York, USA) to deliver a 1mA current for 20 min (including 30 s ramp up and 30 s ramp down). Current was applied transcranially to the right frontal cortex of rat (approximately 2 mm anterior to bregma and 2 mm right to sagittal suture) to obtain similar physiological outcome as that in the human tDCS application studies. An Ag/AgCl wire (d=1.03 mm) used as an active electrode was positioned onto the skull inside a custom built electrode holder (contact area = 12.56 mm<sup>2</sup>, length = 20.22 mm). The electrode holder was uniformly filled with a conductive gel (Signa, NJ, USA). Both active electrode and electrode holder were held in place over the stimulation area using a rotating adjustable clamp and a micromanipulator from Narishige International USA, Inc. (NY, USA). The returning electrode (5x5 cm adhesive conductive fabric electrode) from Axelgaard Manufacturing Co., Ltd. (CA, USA) was placed onto the ventral thoracic region of the anaesthetized rat. Prior to the placement of the returning electrode, hair over the thoracic region was removed and a thin layer of Signa gel was spread to maintain uniform skin-electrode contact.

## 2.4 Multi-photon microscopy and image collection

The microvessels were observed with a 40x lens (water immersion, NA 0.8; Olympus Corporation, Tokyo, Japan), and the 12-bit images were collected by a multi-photon microscopy system (Ultima; Prairie Technologies Inc., Middleton, WI, USA). For all solutes, the excitation wavelength of the multi-photon microscope was set to 840 nm.

After tDCS stimulation for 20 min, the rat was immediately placed under the objective of the multi-photon microscope. The tracer solution (syringe filled with solutes) was then introduced into the cerebral circulation via the carotid artery at a constant flow rate of ~3 mL/min for 1 min in an interval of 5 minutes. Simultaneously, the images of the ROI containing the microvessels and surrounding brain tissue were captured for 1 minute at 5-min intervals up to 25 min. The images of 239 μm x 239 μm (512 x 512 pixels) were collected at a rate of ~1.5 second per image. The corresponding resolution is 0.467 μm x 0.467 μm. The collected images were then transferred to an image acquisition and analysis workstation to determine the BBB solute permeability (**Fig. 2**).

## 2.5 Experimental protocol

**Figure 1D** summarizes the experimental protocol for tDCS stimulation effects on the BBB solute permeability. Cathodal and anodal tDCS was applied at a current strength of 1 mA for 20 min by a constant current stimulator. After stimulation, the rat head was mounted into the multiphoton microscope, and the ROI with cerebral microvessels was found. This took about 10 minutes. Then, the images for determining the BBB solute permeability were collected for 1 min at a rate of one image per second in a 5-minute interval, up to 25 min.

## 2.6 Determination of the BBB solute permeability

We used the similar method as in our previous studies for permeability of pial microvessels<sup>26</sup> to determine permeability of cerebral microvessels ~100–200 μm below the pia mater. Post-capillary venules of 15–40 μm diameter and capillaries were chosen for the permeability measurement<sup>26,27</sup>. The reasons that we currently only measured the permeability of post-capillary venules were: 1) to avoid the influence of smooth muscle cells at arteries, arterioles, and large venules, which would contract under stimuli and affect the permeability measurement<sup>27</sup>; 2) our previous studies on the BBB permeability were also conducted on this type of post-capillary venules<sup>25,26</sup>.

The permeability was determined off-line from the pre-collected images by using ImageJ (National Institutes of Health, Bethesda, MD, USA). **Figure 2A** shows a typical image of an ROI (~239  $\mu\text{m}$  x 239  $\mu\text{m}$ ) with a couple of microvessels and surrounding brain tissue. The total fluorescence intensity in a rectangular window including a vessel lumen and the surrounding tissue was measured by ImageJ. The measuring window was ~50–100  $\mu\text{m}$  long and ~30–60  $\mu\text{m}$  wide and was set at least 10  $\mu\text{m}$  from the base of the bifurcation to avoid solute contamination from the side arms. The criteria for the size and placement of the measuring window were 1) the vessel segment is straight 2) the dye does not spread out of the window during the time for permeability measurement (10–60 seconds), and 3) no dye contamination from the neighboring vessels into the window. When the criteria were satisfied, permeability was determined using the equation<sup>26, 28</sup>,

$$P = 1/\Delta I_0 * (dI/dt)_0 * r/2$$

where  $P$  is microvessel solute permeability,  $\Delta I_0$  is the step increase of the fluorescence intensity in the window when the dye just fills up the vessel lumen,  $(dI/dt)_0$  is the slope of the increasing curve of the total intensity  $I$  versus time  $t$  when the solute further diffuses into the surrounding tissue, and  $r$  is the vessel radius.

### 3. RESULTS

The tDCS current dosage, applied location, and total duration are important factors in controlling the BBB-disruption levels and determining whether the increased BBB permeability is reversible. We set our variables based on prior literature. **Figures 3,4** show the transient effect of tDCS treatment on BBB permeability. **Figures 3Ai** and **Aiii** show the undisrupted post-capillary vessels of control groups injected with sodium fluorescein and FITC-dextran 20k solution, respectively. **Figures 3A-ii** and **-iv** show the images of post-capillary venules 10 minutes after receiving the tDCS treatment injected with sodium fluorescein and FITC-dextran 20k solution, respectively. Though the change in permeability may not be apparent from these static images, the corresponding graphs in **Figure 3A** clearly illustrate differences between the measured permeability values for each image in **Figure 3A**. For sodium fluorescein, the permeability values for control and 10 min after the tDCS treatment shown in **Figure 3Ai,ii** were  $24.7 \times 10^{-7}$  and  $198 \times 10^{-7}$  cm/s, respectively. For FITC-Dex 20k, the permeability values for control and 10 min after the tDCS treatment shown in **Figure 3Aiii,iv** were  $3.39 \times 10^{-7}$  and  $118 \times 10^{-7}$  cm/s, respectively.

**Figure 4** compares the BBB permeability to sodium fluorescein, FITC-Dextran 20k and 70k, under control and treatment of the tDCS (1mA for 20 min). The solid lines in **Figure 4** demonstrate the responses of the BBB permeability to tDCS as a function of time. At 10 min after the 20 min tDCS treatment, the permeability of post-capillary venules increased to  $(242 \pm 25.3) \times 10^{-7}$  (n=8),  $(94.6 \pm 7.95) \times 10^{-7}$  (n=8), and  $(84.3 \pm 17.4) \times 10^{-7}$  cm/s (n=7) for sodium fluorescein, FITC-dextran 20k and 70k, respectively. Compared to the respective control groups, there were significant increases of  $8.26 \pm 0.86$  ( $p < 0.003$ ),  $34.3 \pm 2.88$  ( $p < 0.001$ ), and  $35.1 \pm 7.27$  ( $p < 0.007$ ) fold. At 15 min post-tDCS, permeability started to recover to the control values; after 20 min, permeability completely returned to the value comparable to the control, indicating a transient BBB permeability increase under this tDCS dose treatment. **Table 1** summarizes the cerebral microvessel permeability ( $P$ ) to sodium fluorescein, FITC-Dextran 20k, and FITC-Dextran 70k under control and **Table 2** summarizes corresponding  $P$  at 10, 15 and 20 min post treatment of 20 min 1mM tDCS.

### 4. DISCUSSION

tDCS has been investigated as a treatment method in various neurological and psychiatric disorders. Weak direct current (1-2 mA) administered during tDCS induces change in cortical excitability in the human brain that last for a significant time period<sup>9</sup>. The resulting electric field allows a change in neuronal firing rate of targeted neuronal networks through sub threshold modulation of resting membrane potentials<sup>29</sup>. Thus, tDCS can be used to modulate neuronal network activity to induce changes in neurophysiologic, psycho physiologic and motor activity as a function of targeted brain areas<sup>30</sup>. In a previous study by Iyer, 2005<sup>31</sup>, the frontal cortex stimulation with 2 mA tDCS for 20 min, produced no hazardous neuropsychological measures and merely any pathological waveforms were noticed on EEG. According to Stagg and Nitsche<sup>19, 32</sup>, the effect of tDCS is polarity specific (anodal increases cortical excitability both during and after stimulation whereas cathodal stimulation decrease excitability in the cortical region) and these effects can outlast the stimulation period for several hours, as long as critical stimulation protocols are met. For example, the

physiological aftereffect of tDCS stimulation (1mA for 9-13 min) sustained for up to 90 min<sup>33,34</sup>. Studies performed in animal model suggest that when tDCS of adequate duration is administered, synaptically driven after-effects are induced whereas during stimulation, cortical excitability are induced by nonsynaptic changes of the cells<sup>35</sup>. However, there has been no study on the effects of tDCS on blood-brain barrier permeability. Our current study thus filled this gap for the neurovascular coupling after tDCS treatments. The tDCS parameters used in this study were based on previous clinical applications of tDCS on humans. Due to the limitation of our technique, we cannot simultaneously determine the BBB permeability changes during tDCS treatments.

## 5. CONCLUSIONS

In summary, we used multiphoton microscopy with high spatial resolution to quantitatively assess the BBB permeability changes in individual cerebral microvessels of rats after the tDCS treatment. We found that tDCS can transiently increase the BBB permeability to small and large molecules. Our findings not only elucidated the cellular mechanisms by which tDCS can enhance neural functions, but also suggested a non-invasive, inexpensive, convenient and well-controlled technique for improving drug delivery to the brain. This work was supported by NIH R21EB017510-01.

## REFERENCES

- [1] Abbott, N.J., Ronnback, L., Hansson, E., 2006. Astrocyte-endothelial interactions at the blood-brain barrier. *Nature Reviews Neuroscience* 7:41-53.
- [2] Betz, A.L., Keep, R.F., Beer, M.E., Ren, X.D., 1994. Blood-brain barrier permeability and brain concentration of sodium, potassium, and chloride during focal ischemia. *J Cereb Blood Flow Metab* 14:29-37.
- [3] Yuan, W., Lv, Y., Zeng, M., Fu, B.M., 2008. Non-invasive measurement of solute permeability in cerebral microvessels of the rat. *Microvascular Research* 77:166-173.
- [4] Vykhodtseva, N.I., Hynynen, K., Damianou, C., 1995. Histologic effects of high intensity pulsed ultrasound exposure with subharmonic emission in rabbit brain in vivo. *Ultrasound Med Biol* 21:969-979.
- [5] Hynynen, K., McDannold, N., Vykhodtseva, N., Jolesz, F.A., 2001. Noninvasive MR imaging-guided focal opening of the blood-brain barrier in rabbits. *Radiology* 220:640-646.
- [6] Brown, R.C., Egleton, R.D., Davis, T.P., 2004. Mannitol opening of the blood-brain barrier: regional variation in the permeability of sucrose, but not 86RB+ or albumin. *Brain Res* 1014:221-227.
- [7] Bikson, M., Name, A., Rahman, A., 2013. Origins of specificity during tDCS: anatomical, activity-selective, and input-bias mechanisms. *Front Hum Neurosci* 7, 688. doi:10.3389/fnhum.2013.00688
- [8] Reis, J., Schambra, H.M., Cohen, L.G., Buch, E.R., Fritsch, B., Zarahn, E., Celnik, P.A., Krakauer, J.W., 2009. Noninvasive cortical stimulation enhances motor skill acquisition over multiple days through an effect on consolidation. *Proc. Natl. Acad. Sci. U.S.A.* 106, 1590–1595. doi:10.1073/pnas.0805413106
- [9] Nitsche, M.A., Paulus, W., 2000. Excitability changes induced in the human motor cortex by weak transcranial direct current stimulation. *J. Physiol. (Lond.)* 527 Pt 3, 633–639.
- [10] Laan, M. ter, van Dijk, J.M.C., Stewart, R., Staal, M.J., Elting, J.-W.J., 2014. Modulation of cerebral blood flow with transcutaneous electrical neurostimulation (TENS) in patients with cerebral vasospasm after subarachnoid hemorrhage. *Neuromodulation* 17, 431–436; discussion 436–437. doi:10.1111/ner.12177
- [11] Dutta, A., Jacob, A., Chowdhury, S.R., Das, A., Nitsche, M.A., 2015. EEG-NIRS based assessment of neurovascular coupling during anodal transcranial direct current stimulation--a stroke case series. *J Med Syst* 39, 205. doi:10.1007/s10916-015-0205-7
- [12] Nitsche, M.A., Paulus, W., 2015. Vascular safety of brain plasticity induction via transcranial direct currents. *Neurology* 84, 556–557. doi:10.1212/WNL.0000000000001242
- [13] Lopez-Quintero, S.V., Datta, A., Amaya, R., Elwassif, M., Bikson, M., Tarbell, J.M., 2010. DBS-relevant electric fields increase hydraulic conductivity of in vitro endothelial monolayers. *J Neural Eng* 7, 16005. doi:10.1088/1741-2560/7/1/016005
- [14] Guarienti, F., Caumo, W., Shiozawa, P., Cordeiro, Q., Boggio, P.S., Benseñor, I.M., Lotufo, P.A., Bikson, M., Brunoni, A.R., 2015. Reducing transcranial direct current stimulation-induced erythema with skin pretreatment: considerations for sham-controlled clinical trials. *Neuromodulation* 18, 261–265. doi:10.1111/ner.12230
- [15] Zhao, M., Bai, H., Wang, E., Forrester, J.V., McCaig, C.D., 2004. Electrical stimulation directly induces pre-angiogenic responses in vascular endothelial cells by signaling through VEGF receptors. *J. Cell. Sci.* 117, 397–405. doi:10.1242/jcs.00868

- [16] Long, H., Yang, G., Wang, Z., 2011. Galvanotactic migration of EA.Hy926 endothelial cells in a novel designed electric field bioreactor. *Cell Biochem. Biophys.* 61, 481–491. doi:10.1007/s12013-011-9231-3
- [17] Song, B., Gu, Y., Pu, J., Reid, B., Zhao, Z., Zhao, M., 2007. Application of direct current electric fields to cells and tissues in vitro and modulation of wound electric field in vivo. *Nat Protoc* 2, 1479–1489. doi:10.1038/nprot.2007.205
- [18] Bai, H., Forrester, J.V., Zhao, M., 2011. DC electric stimulation upregulates angiogenic factors in endothelial cells through activation of VEGF receptors. *Cytokine* 55, 110–115. doi:10.1016/j.cyto.2011.03.003
- [19] Stagg, C.J., Lin, R.L., Mezue, M., Segerdahl, A., Kong, Y., Xie, J., Tracey, I., 2013. Widespread modulation of cerebral perfusion induced during and after transcranial direct current stimulation applied to the left dorsolateral prefrontal cortex. *J. Neurosci.* 33, 11425–11431. doi:10.1523/JNEUROSCI.3887-12.2013
- [20] Giorli, E., Tognazzi, S., Briscese, L., Bocci, T., Mazzatenta, A., Priori, A., Orlandi, G., Del Sette, M., Sartucci, F., 2015. Transcranial Direct Current Stimulation and Cerebral Vasomotor Reserve: A Study in Healthy Subjects. *J Neuroimaging* 25, 571–574. doi:10.1111/jon.12162
- [21] Wang, Y., Hao, Y., Zhou, J., Fried, P.J., Wang, X., Zhang, J., Fang, J., Pascual-Leone, A., Manor, B., 2015. Direct current stimulation over the human sensorimotor cortex modulates the brain's hemodynamic response to tactile stimulation. *Eur. J. Neurosci.* 42, 1933–1940. doi:10.1111/ejn.12953
- [22] Mielke, D., Wrede, A., Schulz-Schaeffer, W., Taghizadeh-Waghefi, A., Nitsche, M.A., Rohde, V., Liebetanz, D., 2013. Cathodal transcranial direct current stimulation induces regional, long-lasting reductions of cortical blood flow in rats. *Neurol. Res.* 35, 1029–1037. doi:10.1179/1743132813Y.0000000248
- [23] Krishnamurthy, V., Gopinath, K., Brown, G.S., Hampstead, B.M., 2015. Resting-state fMRI reveals enhanced functional connectivity in spatial navigation networks after transcranial direct current stimulation. *Neurosci. Lett.* 604, 80–85. doi:10.1016/j.neulet.2015.07.042
- [24] Saiote, C., Turi, Z., Paulus, W., Antal, A., 2013. Combining functional magnetic resonance imaging with transcranial electrical stimulation. *Front Hum Neurosci* 7, 435. doi:10.3389/fnhum.2013.00435
- [25] Shi, L.Y., Zeng, M., Sun, Y., Fu, B.M., 2014. Quantification of blood-brain barrier solute permeability transport by multiphoton microscopy. *Journal of biomechanical engineering* 136(3):031005. doi:10.1115/1.4025892
- [26] Yuan, W., Lv, Y., Zeng, M., Fu, B.M., 2009. Non-invasive measurement of solute permeability in cerebral microvessels of the rat. *Microvasc Res* 77(2):166-173.
- [27] Easton, A.S., Sarker, M.H., Fraser, P.A., 1997. Two components of blood-brain barrier disruption in the rat. *J Physiol* 503:613-623.
- [28] Fu, B.M., Shen, S., 2004. Acute VEGF effect on solute permeability of mammalian microvessels in vivo. *Microvasc Res* 68:51-62.
- [29] Brunoni, A.R., Amadera, J., Berbel, B., Volz, M.S., Rizzerio, B.G., Fregni, F., 2011. A systematic review on reporting and assessment of adverse effects associated with transcranial direct current stimulation. *International Journal of Neuropsychopharmacology* 14, 1133–1145. doi:10.1017/S1461145710001690
- [30] Fregni, F., Boggio, P.S., Nitsche, M., Berman, F., Antal, A., Feredoes, E., Marcolin, M.A., Rigonatti, S.P., Silva, M.T.A., Paulus, W., Pascual-Leone, A., 2005. Anodal transcranial direct current stimulation of prefrontal cortex enhances working memory. *Exp Brain Res* 166, 23–30. doi:10.1007/s00221-005-2334-6
- [31] Iyer, M.B., Mattu, U., Grafman, J., Lomarev, M., Sato, S., Wassermann, E.M., 2005. Safety and cognitive effect of frontal DC brain polarization in healthy individuals. *Neurology* 64, 872–875. doi:10.1212/01.WNL.0000152986.07469.E9
- [32] Nitsche MA, Niehaus L, Hoffmann KT, et al. MRI study of human brain exposed to weak direct current stimulation of the frontal cortex. *Clin Neurophysiol* 2004;115:2419–2423
- [33] Nitsche, M.A., Paulus, W., 2001. Sustained excitability elevations induced by transcranial DC motor cortex stimulation in humans. *Neurology* 57, 1899–1901. doi:10.1212/WNL.57.10.1899
- [34] Nitsche, M.A., Nitsche, M.S., Klein, C.C., Tergau, F., Rothwell, J.C., Paulus, W., 2003. Level of action of cathodal DC polarisation induced inhibition of the human motor cortex. *Clinical Neurophysiology* 114, 600–604. doi:10.1016/S1388-2457(02)00412-1
- [35] Marquez-Ruiz, J., Leal-Campanario, R., Sanchez-Campusano, R., Molaei-Ardekani, B., Wendling, F., Miranda, P.C., Ruffini, G., Gruart, A., Delgado-Garcia, J.M., 2012. Transcranial direct-current stimulation modulates synaptic mechanisms involved in associative learning in behaving rabbits. *Proc Natl Acad Sci USA* 109(17): 6710-6715. doi:10.1073/pnas.1121147109

## FIGURES AND CAPTIONS

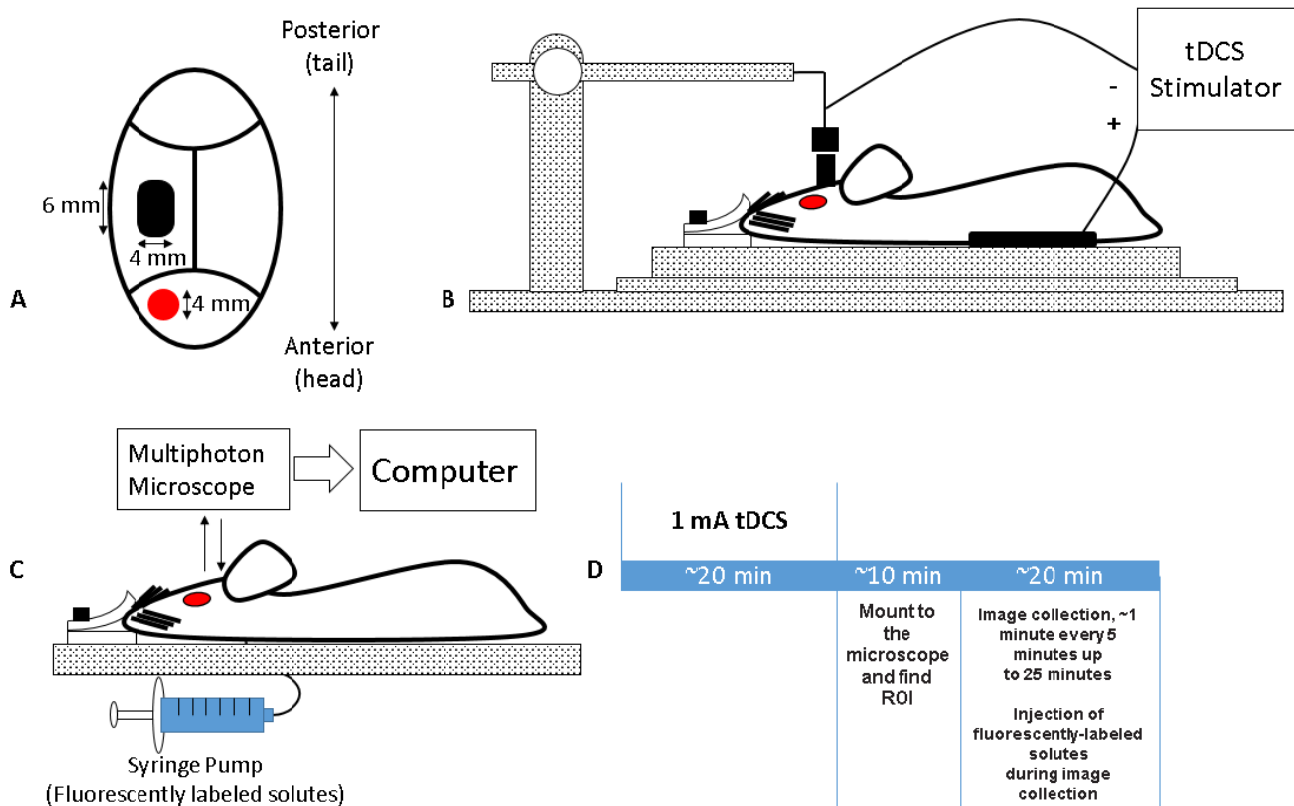


**Figure 1** Illustration of experimental setups.

(A) Schematic of the rat skull for the locations of tDCS treatment and multiphoton imaging. The rectangular black ellipse represents the area of thinned skull that the microscope views. The red circle represents the area of the tDCS application. (B) Schematic of the setup for tDCS application. (C) Schematic of the blood-brain barrier solute permeability measurement by multiphoton microscopy. While solution is injected through the carotid artery at a rate of ~3 mL/min, which is the normal blood flow rate in the artery, the images of the ROI containing several microvessels and the surrounding brain tissue are collected. Permeability is determined off-line by analyzing the collected images. (D) Experimental timeline and protocol for the tDCS treatment and the blood-brain barrier permeability measurement.

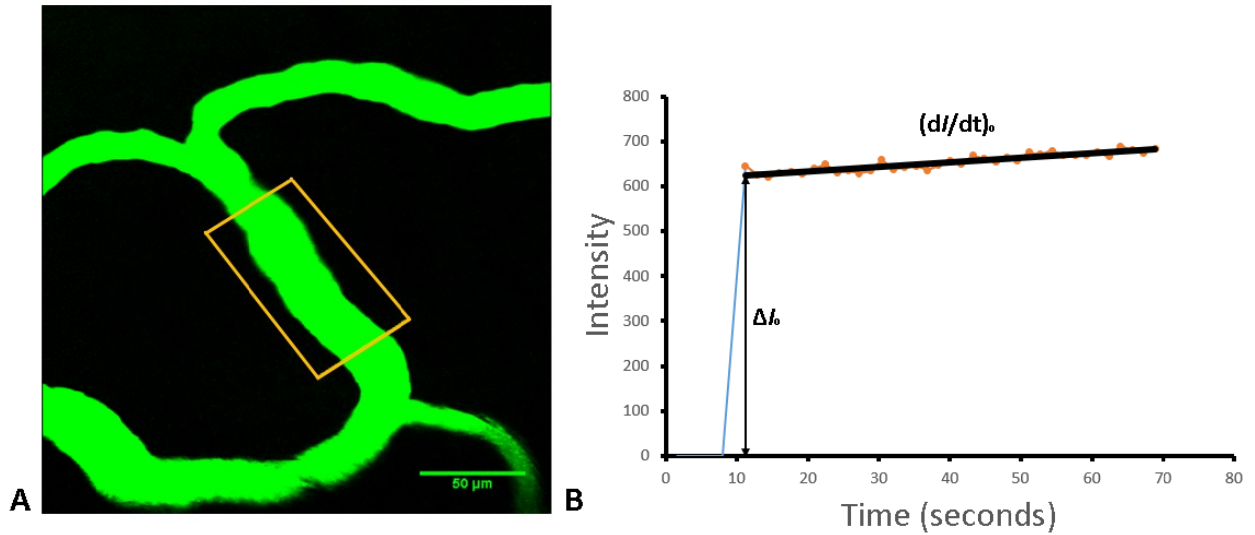


**Figure 2** Determination of the blood-brain barrier solute permeability. **(A)** Illustration of the scanning region comprising several microvessels ~100-200 μm below the pia mater. The imaging area is ~239 μm x 239 μm. The orange frame enclosed area is the region of interest (ROI) used to determine the blood-brain barrier permeability to a solute. **(B)** Total fluorescence intensity in the ROI as a function of perfusion time (blue and red lines). Fluorescence intensity in the ROI is proportional to the total mass of solute accumulated in the measuring region surrounding the microvessel. The slope of the regression line over the initial linear accumulation  $(dI/dt)_0$  (black line) is used to determine permeability  $P = 1/\Delta I_0 * (dI/dt)_0 * r/2$ , where  $\Delta I_0$  (black line with arrowheads) is the step intensity increase when the dye just fills up the vessel lumen, and  $r$  is the radius of the vessel. The vessel shown has a radius of 12 μm and permeability of  $3.57 \times 10^{-7}$  cm/s for FITC-Dex 20k.

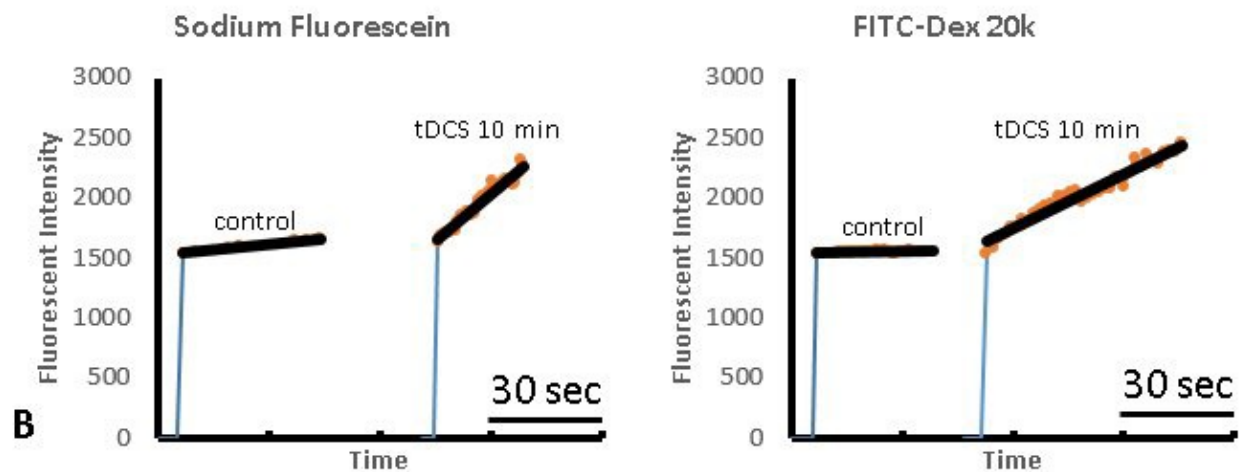
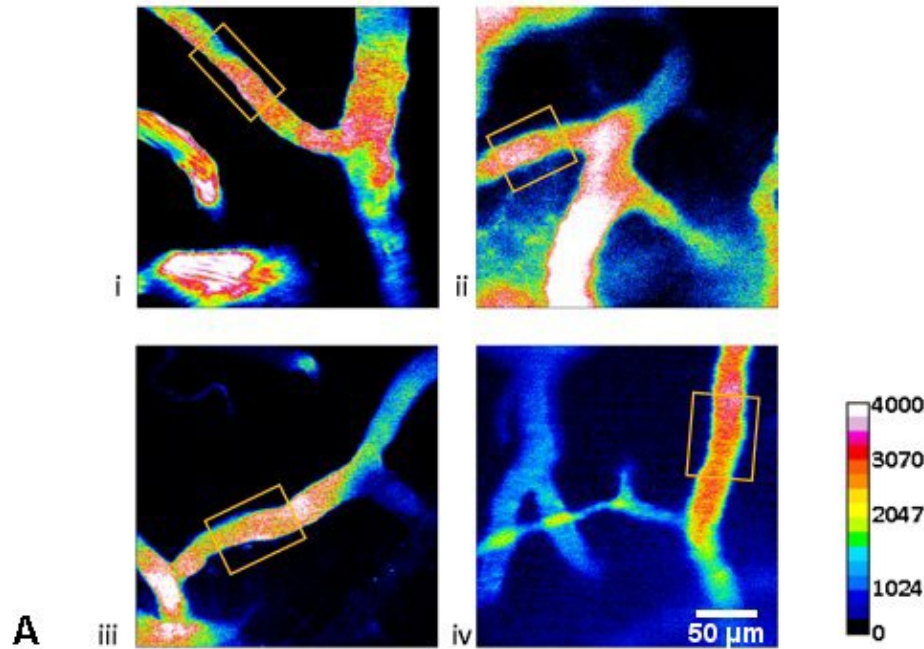


**Figure 3** Representative images of the scanning region under various conditions and their corresponding graphs. (A) i and ii are images for sodium fluorescein under control and 10 min post tDCS treatment, respectively, while iii and iv are those for FITC-Dextran 20k. The ROI's (orange boxes) were chosen from each image to quantify the permeability. (B) Fluorescent intensity vs time graphs of the 4 ROIs from (A). The permeability values for post-capillary venules in **Figs. 3Ai, Aii** are  $24.7 \times 10^{-7}$  ( $r=10.6 \mu\text{m}$ ),  $198 \times 10^{-7}$  ( $r=11.8 \mu\text{m}$ ) cm/s for sodium fluorescein (left graph in **Fig. 3B**) under control and 20 min post tDCS treatment. They are  $3.39 \times 10^{-7}$  ( $r=12.7 \mu\text{m}$ ), and  $118 \times 10^{-7}$  cm/s ( $r=14.8 \mu\text{m}$ ), respectively, for FITC-Dex-20k (right graph in **Fig. 3B**) for vessels shown in **Figs. Aiii, Aiv**.

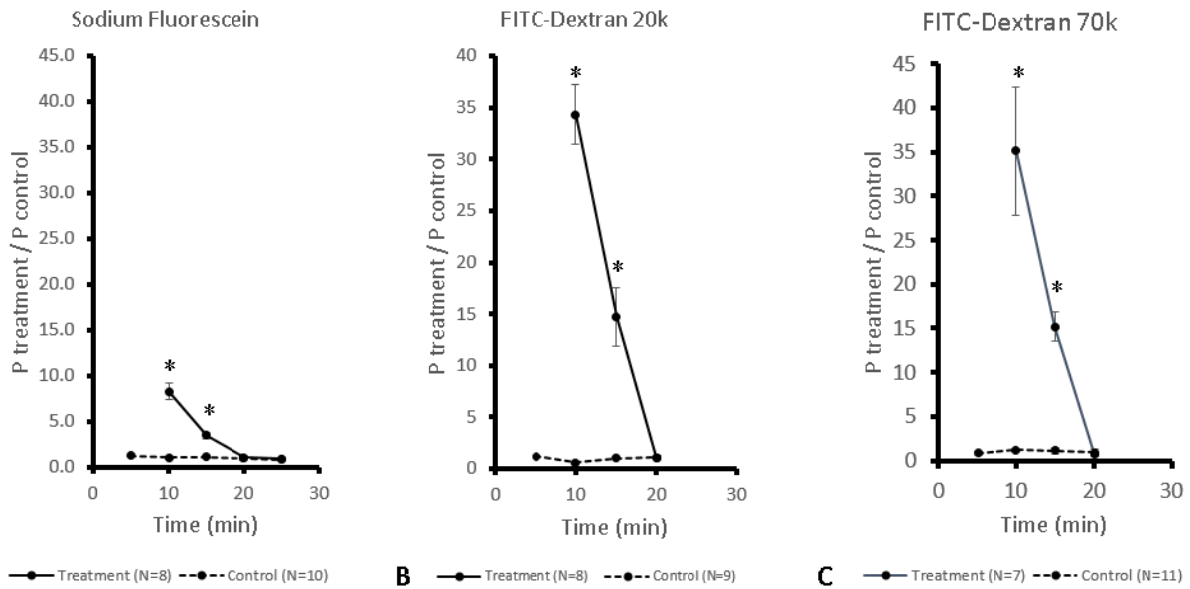


**Figure 4** Normalized blood-brain barrier permeability as a function of time under the control (dashed line) and post treatment of tDCS (solid line) for sodium fluorescein (A), FITC-dex20k (B) and FITC-dex70k (C). \*p-value <0.05 compared with the corresponding control.

## TABLES AND CAPTIONS

**Table 1** Cerebral microvessel permeability (P) to sodium fluorescein, FITC-Dextran 20k, and FITC-Dextran 70k under control treatment

Solute	Number of Vessels	Vessel Diameter mean $\pm$ SE ( $\mu\text{m}$ )	P mean $\pm$ SE ( $\times 10^{-7}$ cm/s)
Sodium Fluorescein	10	19.0 $\pm$ 2.6	29.4 $\pm$ 2.36
FITC-Dextran 20k	9	20.3 $\pm$ 3.8	2.76 $\pm$ 0.32
FITC-Dextran 70k	11	18.4 $\pm$ 0.8	2.4 $\pm$ 0.26

**Table 2** Cerebral microvessel permeability (P) to sodium fluorescein, FITC-Dextran 20k, and FITC-Dextran 70k after 20 min tDCS treatment

Solute	Number of Vessels	Vessel Diameter ( $\mu\text{m}$ )	Time after tDCS treatment (min)	P mean $\pm$ SE ( $\times 10^{-7}$ cm/s)
Sodium Fluorescein	8	22.6 $\pm$ 6.8	10	242 $\pm$ 25.3
			15	101 $\pm$ 9.05
			20	29.1 $\pm$ 1.82
FITC-Dextran 20k	8	22.8 $\pm$ 1.7	10	94.6 $\pm$ 7.96
			15	40.7 $\pm$ 7.83
			20	3.07 $\pm$ 0.48
FITC-Dextran 70k	7	20.1 $\pm$ 3.2	10	84.3 $\pm$ 17.4
			15	36.5 $\pm$ 4.11
			20	1.91 $\pm$ 0.21